Physicochem. Probl. Miner. Process., 54(2), 2018, 590-600

http://www.journalssystem.com/ppmp/

Physicochemical Problems of Mineral Processing

ISSN 1643-1049

Received September 29, 2017; reviewed; accepted November 20, 2017

Effect of calcination temperature on activation behaviors of coal-series kaolin by fluidized bed calcination

Shuai Yuan [1, 2], Yuexin Han [1], Yanjun Li [1, 2], Peng Gao [1], Jianwen Yu [1]

[1] College of Resources and Civil Engineering, Northeastern University, Shenyang 110819, China

[2] Research Center of Coal Resources Safe Mining and Clean Utilization, Liaoning Technical University, Fuxin 123000, China

Corresponding author: dongdafulong@mail.neu.edu.cn (Yuexin Han)

Abstract: This paper is aimed at investigating activation behaviors for coal-series kaolin using fluidized bed calcination as a novel method. The properties of calcined products at different temperature by fluidized bed calcination were evaluated by determination of weight loss rate, whiteness, chemical oxygen demand (COD), aluminum dissolution degree. The thermal behaviors and reaction mechanism were characterized by thermo gravimetric-differential scanning calorimetry (TG-DSC), X-ray diffraction (XRD), Fourier transform infrared spectroscopy (FT-IR), particle size distribution (PSD) and scanning electron microscopy (SEM). The results showed that calcination temperature was essential factor determining the properties and crystallinity of calcined products using fluidized bed calcination. Coal-series kaolin transformed into irregular and amorphous metakaolin with excellent properties as calcined at 600-900 °C, which attributed to the dehydroxylation of kaolinite and combustion of carbon/organic matter. Calcined kaolin eliminated activity ascribed to the recrystallization into mullite when calcination temperature was over 1000 °C. It was believed that fluidized bed calcination was an efficient thermal activation technology for coal-series kaolin and the calcination temperature should be controlled accurately.

Keywords: *coal-series kaolin, fluidized bed calcination, calcination temperature, activation behaviors*

1. Introduction

Coal-series kaolin is an associated resource as tailings in coal mining and washing industry and widely distributed in China. The hard kaolin ore associated with the coal is described as coal-series kaolin. Mass accumulations of the coal-series kaolin have contributed to resource waste and environment deterioration, which has been one of factors restricting sustainable development of resource utilization (Wang et al., 2016). The utilization of coal-series kaolin as resource material will not only decrease pollution to environment, but also bring economic benefits (Qiao et al., 2008). The main components of coal-series kaolin were kaolinite, quartz, carbonaceous matter, organic matter and the other impurities such as iron mineral. Kaolinite ($Al_2O_3 \cdot 2SiO_2 \cdot 2H_2O$) is primary mineral with low activity attributed to 1:1 layer stable crystal structure, which formed by SiO_4 tetrahedral sheets and $AlO_2(OH)_4$ octahedral sheets shown in Fig. 1 (Johnson and Arshad, 2014; Liu and Yang, 2014).

Thermal technology such as calcination is an effective method to activate coal-series kaolin through dehydroxylation of kaolinite and combustion of carbon/organic matter (Liu et al., 2015). The calcined kaolin can be transformed into meta-kaolinite, amorphous SiO_2 and Al_2O_3 after calcination at appropriate temperature (Kuang et al., 2016; Souri et al., 2015; Zhou et al., 2015). And the calcined kaolin has excellent product properties such as high chemical activity, high whiteness and high dissolution degree of aluminum, which can be widely applied the production of paper, functional materials, building materials, and chemical products (Liew et al., 2012; Xu et al., 2015; Zhou et al., 2012). However, the temperatures outside the reasonable ranges could lead to the beginning of

http://dx.doi.org/10.5277/ppmp1862

crystallization, the presence of new stable phase (mullite and cristobalite etc.) and the decreased activity in calcined products (Cao et al., 2016b). Therefore, in order to get high-quality calcined kaolin, the calcination temperature should be controlled accurately (Zhang et al., 2016). Fluidized bed technology is easier for controlling, realizing large-scale, higher efficiency on heat and mass transfer process, and better bed temperature distribution than traditional devices (Khadilkar et al., 2014; Scala and Salatino, 2003; Zhang, 2009). High-performance fluidized bed technology has been widely used in chemical engineering, curatorial industry and other fields. Zeng et al. (2015) has made successful extraction of vanadium from stone coal by roasting in a fluidized bed reactor. Li and Zhu (2012) has achieved high recovery of low grade hematite via fluidized bed magnetizing roasting. The fluidized bed technology was considered to have great potential to thermal treatment of ore at large scale. However, the study of fluidized bed technology applied in calcination process of coal-series kaolin has been rarely reported.

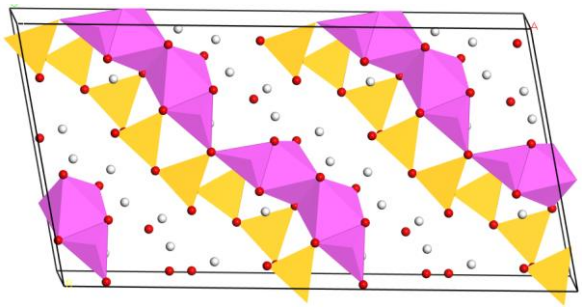

Fig. 1. Crystal structure of kaolinite (Element color: white =H; red=O; purple=Al; yellow= Si)

The purpose of this paper is to present fluidized bed calcination applying to activation of coal-series kaolin and investigate the influence of calcination temperature on activation behaviors of calcined products by the novel method. The properties of calcined products such as weight loss rate, whiteness, chemical oxygen demand and dissolution degree of aluminum were investigated. Furthermore, the thermal behaviors and reaction mechanism were discussed by means of TG-DSC, XRD, FT-IR, PSD and SEM. This research has important significance for comprehensive utilization of coal-series kaolin with large scale, high-efficiency production of calcined kaolin with excellent properties and development of new fluidized bed equipment at reasonable calcination temperature.

2. Materials and methods

2.1 Minerals

The raw coal-series kaolin used in this study was collected from Shuozhou (Shanxi Province, China). The raw coal-series kaolin is wet ultrafine ground on which we then conducted the Chemical compositions, XRD, SEM, and PSD analysis. Chemical compositions analysis of coal-series kaolin was carried out and shown in Table 1. It is clearly evident that the raw coal-series kaolin samples consist of Al_2O_3 (37.83%) and SiO_2 (47.38%), respectively. X-ray diffraction patterns were used to determine the mineral composition of raw coal-series kaolin and the results were shown in Fig. 2. It indicates kaolinite ($Al_2O_3 \cdot 2SiO_2 \cdot 2H_2O$) and quartz ($SiO_2$) are the major crystallized minerals presented in the raw coal-series kaolin. SEM image and EDS spectra of raw coal-series kaolin were measured and shown in Fig. 3. The results show that the raw coal-series kaolin has a high purity of 95.69% kaolinite, which can be calcined to prepare a high reactive calcined kaolin. Particle size distribution of raw coal-series kaolin was investigated and shown in Fig. 4. The result indicates that the raw coal-series kaolin particle was milled to 85% passing 15 μm during the wet ultrafine grinding by stirred mill.

Table 1. Chemical compositions of raw coal-series kaolin (wt%)

Al_2O_3	SiO_2	Fe_2O_3	TiO_2	CaO	MgO	C	P	S	LOI
37.83	47.38	0.24	0.39	0.04	0.12	1.68	0.011	0.027	14.74

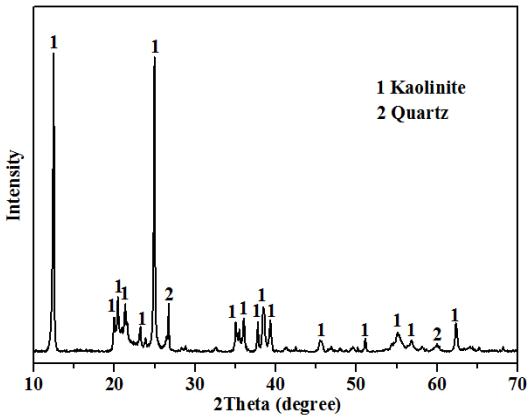

Fig. 2. X-ray diffraction spectra of raw coal-series kaolin

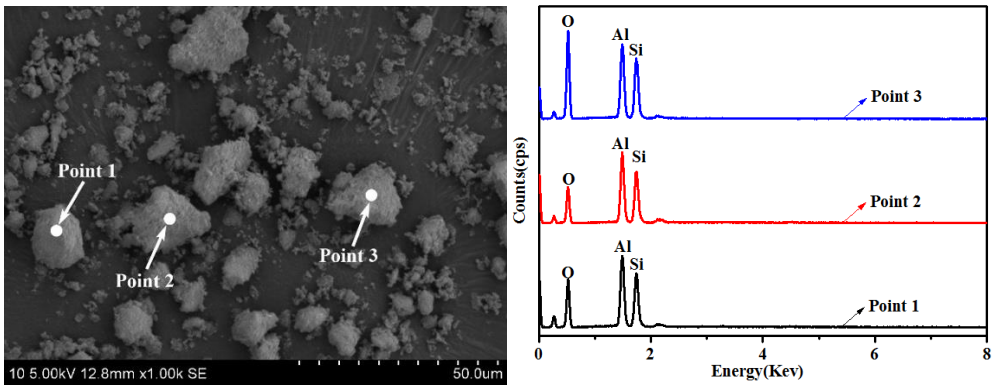

Fig. 3. SEM image and EDS spectra of raw coal-series kaolin

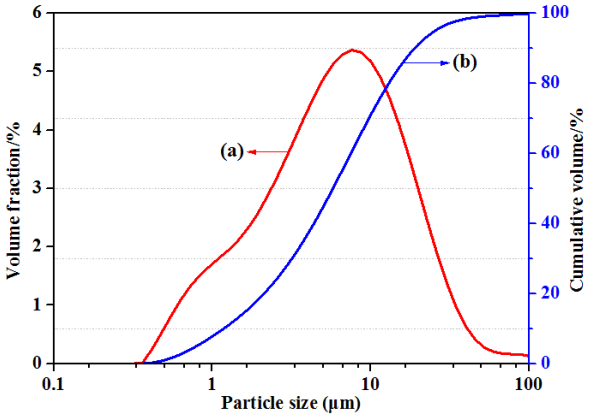

Fig. 4. Particle size distribution of coal-series kaolin, (a) volume fraction, (b) cumulative volume

2.2 Apparatus and procedure

The fluidized bed calcination experiments were performed in a customized bench-scale fluidized bed as shown in Fig. 5. The fluidized bed apparatus consists of a fluidized bed reactor, an electric furnace, a temperature controller and a gas supply system. The fluidized bed reactor was made of high purity quartz glass and was 25 mm in inner diameter. Experiment was started by feeding exactly 15 g samples and heating the reactor to a desired temperature with the rate of 10 °C/min, and then high-purity air at a constant flow rate of 800 cm^3/min was fed into the reactor to form the roasting atmosphere. The sample was dry grinding for −15 μm occupying 85% of the specific surface area of 1.99 m^2/g with minimum fluidization velocity of 0.07 m/s. After calcination 180min, the fluidized bed reactor was cooled quickly to the room temperature with nitrogen and the samples were taken out for analysis.

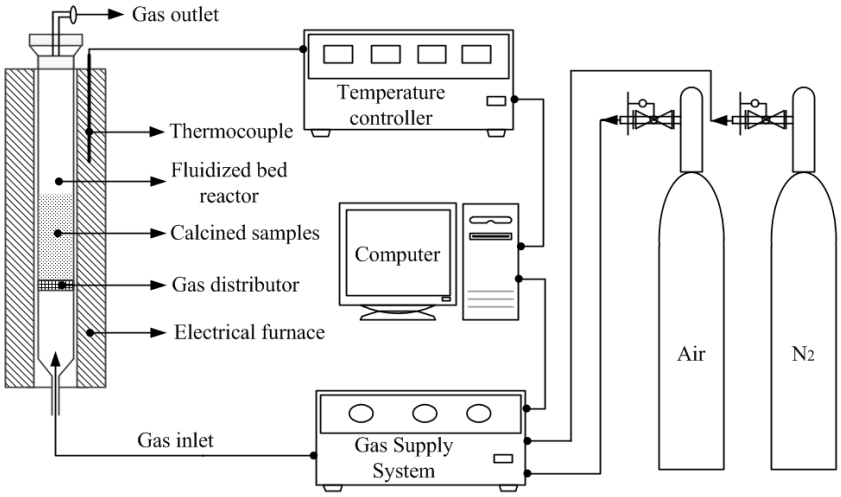

Fig. 5. Schematic diagram of the bench-scale fluidized bed reactor

2.3 Property test methods

The weight loss rate of calcined kaolin was calculated with the formula

$$\alpha = \frac{M_0 - M_T}{M_0 - M_f}$$

where α was weight loss rate, M_0 was the mass of samples before calcination, M_T was the mass of samples after calcination at desired temperature, M_f was final mass of samples after reaction completely.

The whiteness was an important index of the calcined kaolin, which should reach a certain standard to produce paper making or substitute part titanium pigment in some fields (Chen et al., 2014). The whiteness of calcined kaolin was investigated using the whiteness meter WSB-2 (XinRui Instruments & Meters CO., LTD. ShangHai, China).

The burnout level of carbon and organic matter in coal-series kaolin can be measured by the chemical oxygen demand (COD). The COD of calcined products should satisfy requirement of no more than 2700 μg/g, which can be applying in functional materials such as glass fiber. The COD value of calcined kaolin was measured by sulfuric acid dichromate method according to the National Standard of China (JC/T 2156-2012).

The dissolution degree of aluminum in hydrochloric acid served as the index of evaluating the activation efficiency of calcined kaolin (Guo et al., 2014; 2015). The leaching processes were as follows: 8 g of calcined kaolin was added to 200 cm^3 agitated HCl solution in a 3-mouth flask, the flask was heated to 90 °C and stirred for 60 min by magnetic stirrers with 900 rpm. Then the mixture was filtered and washed with deionized water many times, the filtrate was analyzed to determine aluminum by inductively coupled plasma atomic emission spectrometer (ICP-AES) and the dissolution degree of aluminum from calcined kaolin was calculated (Cui et al., 2015).

2.4 TG-DSC measurement

The thermal behavior of coal-series kaolin was analyzed by thermogravimetric-differential scanning calorimetry (TG-DSC) using a thermal analyzer (Netzsch Scientific Instruments Trading Ltd., SelbCity, Germany). The TG-DSC analysis was performed at the air or nitrogen atmosphere with a flow rate of 50 cm^3/min and heated from room temperature to 1200 °C at constant heating rate of 10 °C/min.

2.5 XRD measurement

Detailed mineralogical phase information of calcined products was obtained by X-ray diffraction (XRD) analysis using PANalytical X'pert PW3040 (PANalytical B.V. Ltd., Almelo, Netherlands). The XRD measurement was operating at 40 kV, 30 mA; diffraction angle range of 2θ was from 10° to 90° with a step of 0.02° (2θ) and a scanning rate of 12°/min.

2.6 FT-IR spectra measurement

The Fourier transform infrared spectroscopy (FT-IR) analysis was carried out by Nicolet 380 FT-IR spectrometer (Thermo Fisher Scientific Ltd. Manufacturer, Waltham City, America Country) to further probe the structure transformation (Liew et al., 2012). 1 mg sample accompanied with 100 mg KBr usually and the spectra were recorded in the range of 4000–500 cm^{-1}.

2.7 PSD measurement

Particle size distribution (PSD) was measured by using a laser particle size analyzer on a Mastersizer 2000 (Malvern Instruments Ltd., UK). Samples were feed into a flask with 500 cm^3 deionized water and agitated at 3000 rpm. Ultrasound dispersion was applied for 5 min prior to measurement. In feeding the particle size analyzer, the suspension was incrementally transferred to the sample cell until the laser obscuration reached 10% (Liang et al., 2017). At least three measurements were made and the average was calculated.

2.8 SEM measurement

The microstructure and morphologies were observed by scanning electron microscope (SEM) using S-3400N (Hitachi, Ltd., Tokyo, Japan). The samples were coated with gold using a sputter coater to increase conductivity prior to SEM characterization.

3. Results and discussion

3.1 TG-DSC analysis

In order to study thermal behaviors of coal-series kaolin, TG-DSC analysis was conducted and shown in Fig. 6. According to literature reports (Ilic et al., 2016), there are three main stages of thermal decomposition for coal-series kaolin, it is respectively the dehydration stage, the organic carbon/organic matter combustion stage and the dehydroxylation of kaolinite stage. Thermal analysis of coal-series kaolin in absence of oxygen shown in Fig. 6(b), the weight loss of 13.65% is attributed to the dehydration and the dehydroxylation of kaolinite. And the combustion of carbon and organic matter causes the weight loss to increase by 2.37% under air flow shown in Fig. 6(a).

The endothermic peak presented at 490 °C in Fig. 6 is contributed by the dehydroxylation of kaolinite and formation of meta-kaolinite according to reaction:

$$Al_2O_3 \cdot 2SiO_2 \cdot 2H_2O \xrightarrow{450°C} Al_2O_3 \cdot 2SiO_2 + 2H_2O_{(g)}. \quad (1)$$

The exothermic peak at 1010 °C is due to the transformation of meta-kaolinite into crystallized mullite ($3Al_2O_3 \cdot 2SiO_2$) according to reaction:

$$3(Al_2O_3 \cdot 2SiO_2) \xrightarrow{1000°C} 3Al_2O_3 \cdot 2SiO_2 + 4SiO_2. \quad (2)$$

The exothermic peak at 580 °C in Fig. 6(a) may be caused by the combustion of carbon and organic matter, the exothermic peak at 615 °C in Fig. 6(b) may be caused by the pyrolysis of the organic matter.

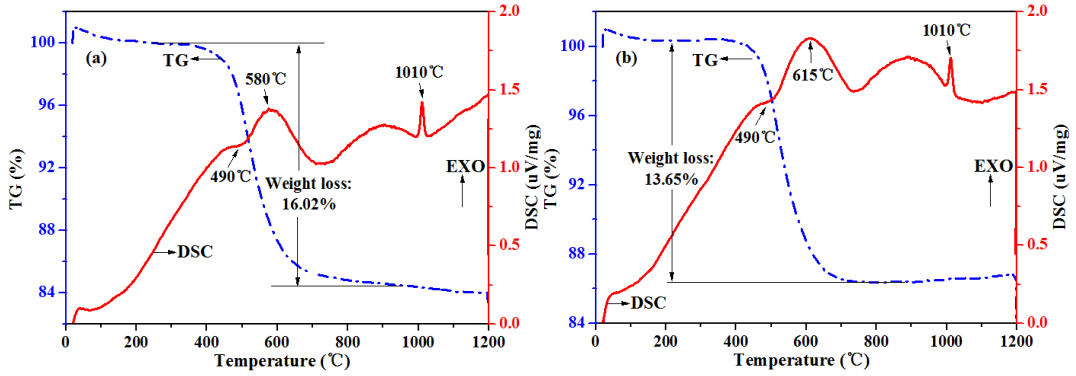

Fig. 6. TG-DSC curves of raw coal-series kaolin, (a) under air flow, (b) under nitrogen flow

3.2 Property of products

The weight loss rate linearly increases with increasing temperature from 400 to 600 °C and remains stable with increasing temperature over 600 °C shown in Fig. 7(a). It can be observed in Fig. 7(b) that the whiteness of kaolin increased with the increasing calcination temperature. But the highest whiteness was obtained after 900 °C, this is mainly due to most of the carbon and organic matter was burnt out with the increasing of calcination temperature. COD values decreased as the calcination temperature increased shown in Fig. 7(c). As the temperature continued to increase, COD value of the calcined product was decreased to 2217 μg/g at 500 °C could approach to the industry standard (2700 μg/g). The COD value could reduce to 460 μg/g with the rise of the temperature to 900 °C. The results could be attributed to the combustion of carbonaceous/organic matter and dehydroxylation of kaolinite and was consistent with the foregoing TG-DSC analysis. However, few fine carbonaceous and organic matters are closely associated with kaolinite in the coal-series kaolin and required higher temperature to burn out. Fig. 7(d) shows the aluminum dissolution degree of calcined kaolin using hydrochloric acid leaching. The aluminum dissolution degree increased with increasing temperature and reached 60% above at 600-900°C, however, the aluminum dissolution degree declined to nearly zero at 1000°C, which was due to the transformation of meta-kaolinite into stable phase mullite with low activity.

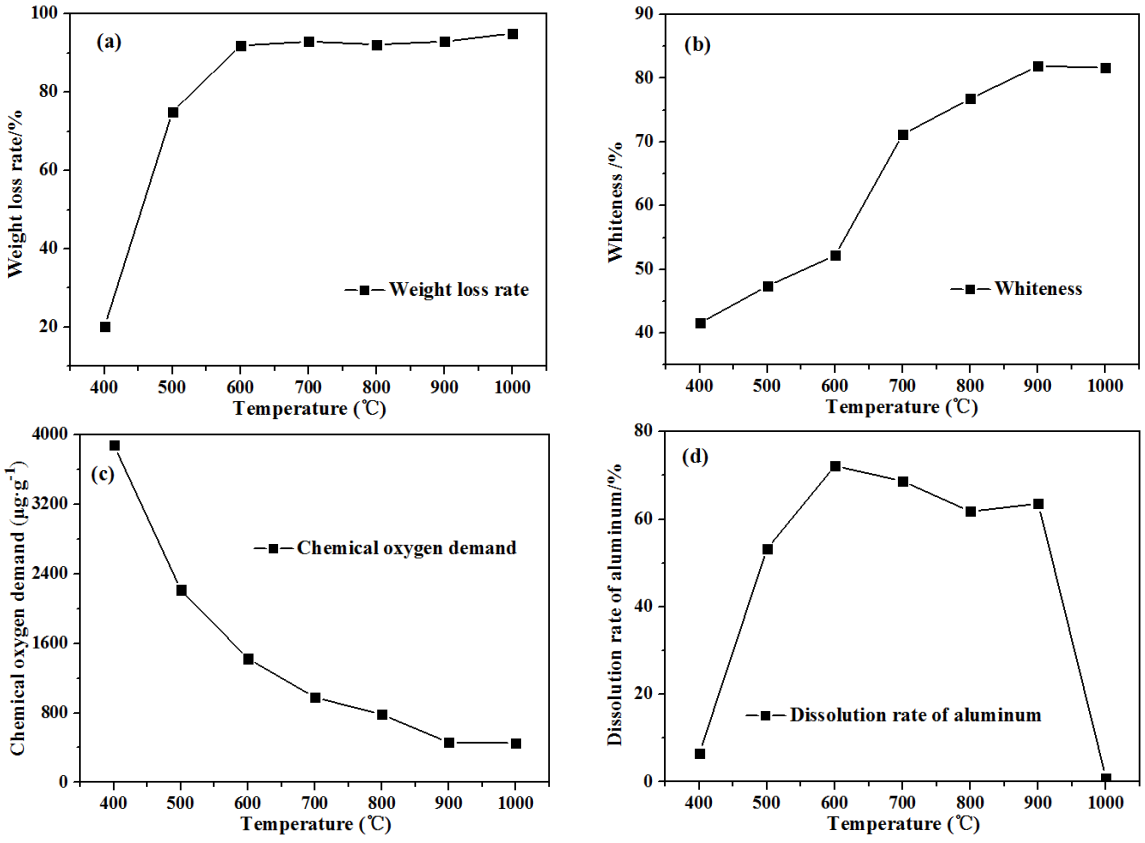

Fig. 7. Product properties of calcined kaolin at different temperature by fluidized bed calcination, (a) weight loss rate, (b) whiteness, (c) chemical oxygen demand, (d) dissolution degree of aluminum

3.3 XRD analysis

Fig. 8 presents the XRD patterns of calcined product at different temperature. The presence of kaolinite can be evaluated by the broadening of the 2-Theta=10-30° peak, particularly the two primary peaks of kaolinite at 12.53° with (001) surface and 25.14° with (011) surface as shown in Fig. 8(b). The decrease and disappearance of peaks at 12.53° and 25.14° suggests a significant breaking in the crystallinity, primarily because the kaolinite transformed into meta-kaolinite with the increase temperature to 600 °C. As show in Fig. 8(a), the kaolinite in calcined coal-series kaolin becomes completely amorphous from 600 °C, the amorphous hump in the spectra growing from 600 °C to

900 °C. And the amorphous meta-kaolinite can achieve high dissolution degree of aluminum in harmony with the results of section 3.1. Meanwhile, the intensity of diffraction peak of quartz at 26.66° with (011) surface increased obviously and the peak at 20.87° with (100) surface gradually emerged as shown in Fig. 8(a). Remarkably, the peak of mullite can be observed at 1000°C, mainly because the amorphous meta-kaolinite transformed to new stable crystal mullite phase ($3Al_2O_3 \cdot 2SiO_2$) with low activities as mentioned in the previous thermal analysis. The mullite phase has contributed to the precipitous decline of aluminum dissolution degree of calcined products at 1000 °C.

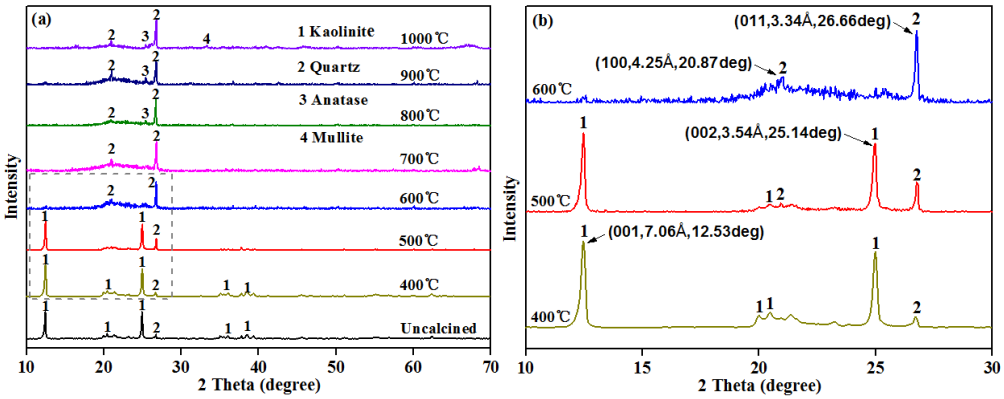

Fig. 8. XRD patterns of calcined product at different temperature by fluidized bed calcination

3.4 FT-IR analysis

Structural characterization of calcined products at different temperature is displayed in Fig. 9. According to current research (Hollanders et al., 2016), kaolinite exhibits distinctive bands in the OH stretching region, 3700-3600 cm^{-1}. As shown in Fig. 9, the band near 3620 cm^{-1} represents the inner OH groups, and the other bands near 3695 cm^{-1} originate from internal octahedral surface OH groups, the two distinctive bands can be seen in uncalcined coal-series kaolinite. The intensities of the bands at 3669 cm^{-1} and 3653 cm^{-1} tend to weaken with increasing of temperature and eventually disappear over 600°C, which suggests that temperature below 500°C is not sufficient for the dehydroxylation by fluidized bed calcination. The bands of 916 cm^{-1} (Al-O-H bands), 803 and 755 cm^{-1} (OH-bands), 696 and 540 cm^{-1} (Si-O-Al^{vi} vibrations) disappeared, indicating the dehydroxylation of kaolinite and transformation of meta-kaolinite. The appearance of new vibration at 809 cm^{-1} can be connected with the change from octahedral coordination of Al in kaolinite to tetrahedral coordination in meta-kaolinite (Fitos et al., 2015).

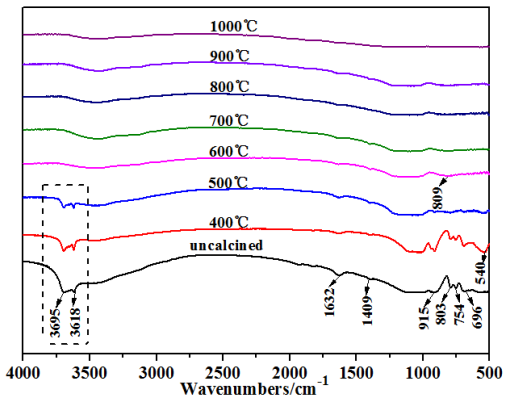

Fig. 9. FT-IR spectra of coal-series kaolin at different temperature by fluidized bed calcination

3.5 PSD analysis

Particle size distribution of the raw coal-series kaolin and calcined kaolin at different temperature are observed in Fig. 10, the mean particle size (D_{50}) is depicted in Fig. 11. As shown in Fig. 10, particle size

distribution of coal-series kaolin is shifted to coarser particles after fluidized bed calcination, thus indicating that fluidized bed calcination caused partial aggregation of smallest particles (Ilic et al., 2016). The mean particle size (D_{50}) of the coal-series kaolin is increased from 5.77 μm to 22.49 μm under 400 °C, and keep stable at about 29 μm under 500~1000 °C as presented in Fig. 11.

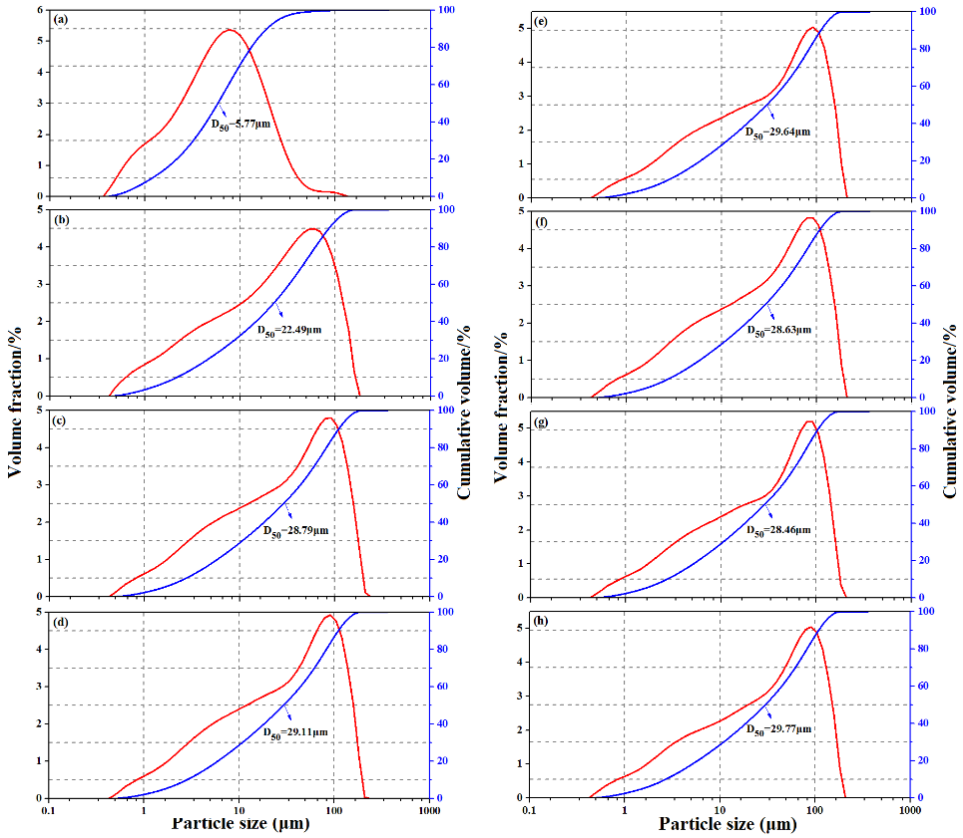

Fig. 10. Particle size distribution of calcined products at different temperatures by fluidized bed calcination, (a) uncalcined, (b) 400, (c) 500, (d) 600, (e) 700, (f) 800, (g) 900, (h) 1000 °C

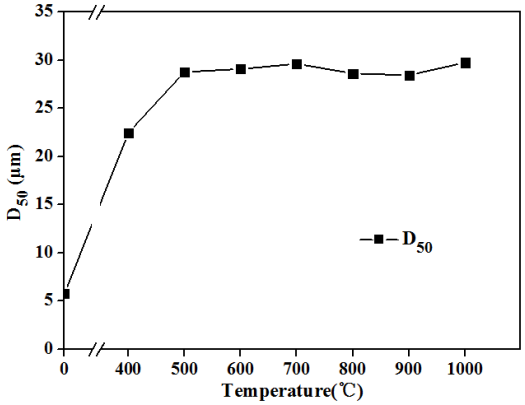

Fig. 11. Mean particle size (D_{50}) of calcined products at different temperatures by fluidized bed calcination

3.6 SEM analysis

For better understanding of the morphology and the physical properties of calcined products by fluidized bed calcination under different temperature, the microstructural evolution was studied using SEM shown in Fig. 12. With increasing temperature, more scale-shaped lamellar structures separate from the group particles by the heat airflow, and turns to irregular and porous by the fluidized bed calcination from 600 to 800 °C. The structure of the $AlO_2(OH)_4$ octahedral layer was destroyed, while the SiO_4 tetrahedron preserved the original lamellar structure, which made the meta-

kaolinite maintain the majority of lamellar structures (Cao et al., 2016a). We could confirm that the dissolution degree and react activity of calcined kaolin mainly depend on the non-crystallizing degree of kaolinite after calcination, which is consistent with reported results in Section 3.2,

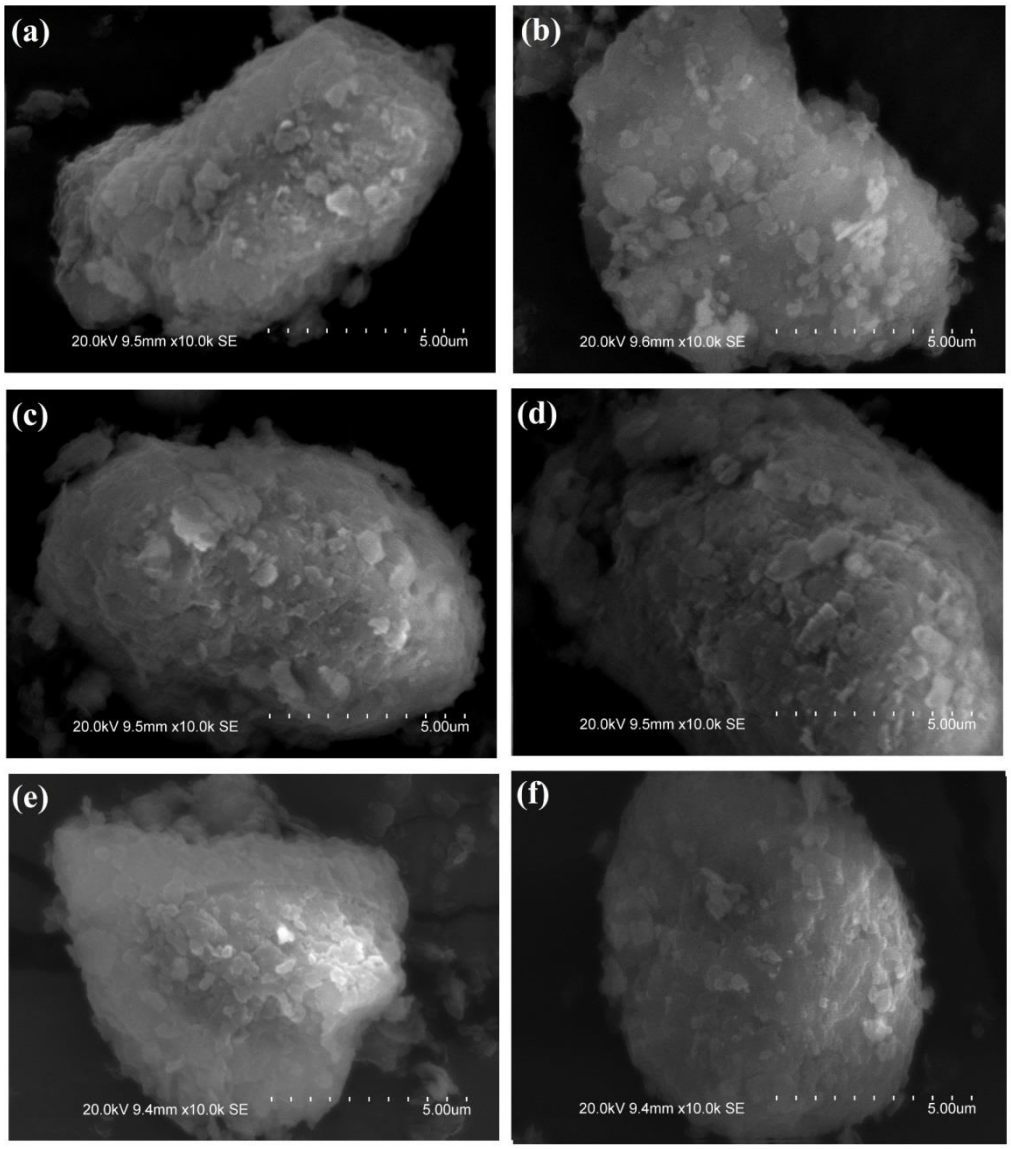

Fig. 12.SEM images of calcined kaolin at different temperatures by fluidized bed calcination, (a) 500 (b) 600, (c) 700, (d) 800, (e) 900, (f) 1000 °C

4. Conclusions

In a present study, properties, phase transformation and microstructure evolution of calcined products by fluidized bed calcination with elevating temperature were investigated and these following conclusions could be drawn:

Kaolinite in coal-series kaolin transformed into meta-kaolinite at 490 °C, meta-kaolinite recrystallized into mullite at 1010 °C according to TG-DSC analysis. The weight loss rate and the whiteness increased with temperature, chemical oxygen demand (COD) decreased gradually and declined to800μg/g with temperature after 900 °C. The calcined kaolin had higher activity at 600-900 °C with higher aluminum dissolution degree and lost activity at 1000 °C.

The diffraction peaks of kaolinite in coal-series kaolin vanish at 600 °C because of its transformation to meta-kaolinite, which can be proved by the disappearance of OH stretching vibration peaks of kaolinite in FT-IR analysis, Meanwhile, new crystalline phase mullite emerged after 1000 °C. Particle size distribution of coal-series kaolin is shifted to coarser particles after fluidized bed

calcination attributed to partial aggregation of smallest particles. Morphology observation proves that the lamellar structure of kaolinite is destroyed into an irregular and porous phase at 500-900 °C and then transforms into a crystalline structure after 1000°C.

The fluidized bed calcination is an efficient thermal activation technology to obtain calcined kaolin with excellent properties at ideal temperature field.

Acknowledgments: This work was funded by the Open Projects of Research Center of Coal Resources Safe Mining and Clean Utilization, Liaoning (LNTU16KF14) and Natural Science Foundation of China (51674064; 51674065).

References

CAO, W., XIA, G.H., LU, M., Huang, H.G., Xu, Y.X., 2016a. *Iron removal from kaolin using binuclear rare earth complex activated thiourea dioxide*. Appl Clay Sci 126, 63-67.

CAO, Z., CAO, Y.D., DONG, H.J., ZHANG, J.S., SUN, C.B., 2016b. *Effect of calcination condition on the microstructure and pozzolanic activity of calcined coal gangue*. Int J Miner Process 146, 23-28.

CHEN, Y.T., ZHOU, C.Y., ALSHAMERI, A., Zhou, S., MA, Y.A., SUN, T., LIAMG, H., GONG, Y.S., WANG, H.Q., YAN, C.J., 2014. *Effect of rice hulls additions and calcination conditions on the whiteness of kaolin*. Ceram Int 40, 11751-11758.

CUI, L., GUO, Y., WANG, X., DU, Z., CHENG, F., 2015. *Dissolution kinetics of aluminum and iron from coal mining waste by hydrochloric acid*. Chinese J Chem Eng 23, 590-596.

FITOS, M., BADOGIANNIS, E.G., TSIVILIS, S.G., PERRAKI, M., 2015. *Pozzolanic activity of thermally and mechanically treated kaolins of hydrothermal origin*. Appl Clay Sci 116, 182-192.

GUO, Y., LV, H., YANG, X., CHENG, F., 2015. *AlCl3·6H2O recovery from the acid leaching liquor of coal gangue by using concentrated hydrochloric inpouring*. Sep Purif Technol 151, 177-183.

GUO, Y.X., YAN, K.Z., CUI, L., CHENG, F.Q., LOU, H.H., 2014. *Effect of Na2CO3 additive on the activation of coal gangue for alumina extraction*. Int J Miner Process 131, 51-57.

HOLLANDERS, S., ADRIAENS, R., SKIBSTED, J., CIZER, O., ELSEN, J., 2016. *Pozzolanic reactivity of pure calcined clays*. Appl Clay Sci 132, 552-560.

ILIC, B., RADONJANIN, V., MALESEV, M., ZDUJIC, M., MITROVIC, A., 2016. *Effects of mechanical and thermal activation on pozzolanic activity of kaolin containing mica*. Appl Clay Sci 123, 173-181.

JC/T2156, 2012. *Determination of COD in Raw Material and Batch of Fiber Glass*. MIIT, Beijing, pp, 1-3.

JOHNSON, E.B.G., ARSHAD, S.E., 2014. *Hydrothermally synthesized zeolites based on kaolinite: A review*. Appl Clay Sci 97-98, 215-221.

KHADILKAR, A., ROZELLE, P.L., PISUPATI, S.V., 2014. *Models of agglomerate growth in fluidized bed reactors: Critical review, status and applications*. Powder Technol 264, 216-228.

KUANG, J., YUAN, W., Li, L., HU, J., XU, L., 2016. *Effects of Er(NO3)3, Nd(NO3)3 and Y(NO3)3 on kinetics of dehydroxylation of kaolinite*. Powder Technol 301, 581-589.

LI, Y., ZHU, T., 2012. *Recovery of low grade haematite via fluidised bed magnetising roasting: investigation of magnetic properties and liberation characteristics*. Ironmak Steelmak 39, 112-120.

LIANG, L., WANG, L., NGUYEN, A.V., XIE, G., 2017. *Heterocoagulation of alumina and quartz studied by zeta potential distribution and particle size distribution measurements*. Powder Technol 309, 1-12.

LIEW, Y.M., KAMARUDIN, H., MUSTAFA Al BAKRI, A.M., LUQMAN, M., KHAIRUL NIZAR, I., RUZAIDI, C.M., HEAH, C.Y., 2012. *Processing and characterization of calcined kaolin cement powder*. Constr Build Mater 30, 794-802.

LIU, S.Y., YANG, H.M., 2014. *Stearic acid hybridizing coal-series kaolin composite phase change material for thermal energy storage*. Appl Clay Sci 101, 277-281.

LIU, X.X., LIU, X.W., HU, Y.H., 2015. *Investigation of the thermal behaviour and decomposition kinetics of kaolinite*. Clay Miner 50, 199-209.

QIAO, X.C., SI, P., YU, J.G., 2008. *A Systematic Investigation into the Extraction of Aluminum from Coal Spoil through Kaolinite*. Environ Sci Technol 42, 8541-8546.

SCALA, F., SALATINO, P., 2003. *Dolomite attrition during fluidized-bed calcination and sulfation*. Combust Sci Technol 175, 2201-2216.

SOURI, A., GOLESTANI-FARD, F., NAGHIZADEH, R., VEISEH, S., 2015. *An investigation on pozzolanic activity of*

Iranian kaolins obtained by thermal treatment. Appl Clay Sci 103, 34-39.

WNANG, Z., FENG, P.Z., WANG, X.H., GENG, P., AKHTAR, F., ZHANG, H.F., 2016. Fabrication and properties of freeze-cast mullite foams derived from coal-series kaolin. Ceram Int 42, 12414-12421.

XU, X.H., LAO, X.B., WU, J.F., ZHANG, Y.X., XU, X.Y., LI, K., 2015. *Microstructural evolution, phase transformation, and variations in physical properties of coal series kaolin powder compact during firing*. Appl Clay Sci 115, 76-86.

ZENG, X., WANG, F., ZHANG, H.F., CUI, L.J., YU, J., XU, G.W., 2015. *Extraction of vanadium from stone coal by roasting in a fluidized bed reactor*. Fuel 142, 180-188.

ZHANG, W., 2009. *A Review of Techniques for the Process Intensification of Fluidized Bed Reactors*. Chinese J Chem Eng 17, 688-702.

ZHANG, Z.H., ZHU, H.J., ZHOU, C.H., WANG, H., 2016. Geopolymer from kaolin in China: An overview. Appl Clay Sci 119, 31-41.

ZHOU, C.C., LIU, G.J., FANG, T., LAM, P.K.S., 2015. Investigation on thermal and trace element characteristics during co-combustion biomass with coal gangue. Bioresource Technol 175, 454-462.

ZHOU, C.C., LIU, G.J., YAN, Z.C., FANG, T., WANG, R.W., 2012. Transformation behavior of mineral composition and trace elements during coal gangue combustion. Fuel 97, 644-650.